



CHEMISTRY & SUSTAINABILITY

# CHEM **SUS** CHEM

ENERGY & MATERIALS

## Accepted Article

**Title:** Effects of Electrolyte Anions on the Reduction of Carbon Dioxide to Ethylene and Ethanol on Copper (100) and (111) Surfaces

**Authors:** Yun Huang, Cheng Wai Ong, and Boon Siang Yeo

This manuscript has been accepted after peer review and appears as an Accepted Article online prior to editing, proofing, and formal publication of the final Version of Record (VoR). This work is currently citable by using the Digital Object Identifier (DOI) given below. The VoR will be published online in Early View as soon as possible and may be different to this Accepted Article as a result of editing. Readers should obtain the VoR from the journal website shown below when it is published to ensure accuracy of information. The authors are responsible for the content of this Accepted Article.

**To be cited as:** *ChemSusChem* 10.1002/cssc.201801078

**Link to VoR:** <http://dx.doi.org/10.1002/cssc.201801078>

WILEY-VCH

[www.chemsuschem.org](http://www.chemsuschem.org)

A Journal of



# Effects of Electrolyte Anions on the Reduction of Carbon Dioxide to Ethylene and Ethanol on Copper (100) and (111) Surfaces

Yun Huang,<sup>[a]</sup> Cheng Wai Ong,<sup>[a]</sup> and Boon Siang Yeo<sup>\*[a]</sup>

**Abstract:** The CO<sub>2</sub> electroreduction reaction has been investigated on Cu(100) and Cu(111) surfaces in 0.1 M KClO<sub>4</sub>, KCl, KBr and KI electrolytes. The formation of ethylene (C<sub>2</sub>H<sub>4</sub>) and ethanol (EtOH) products on these surfaces generally increased as the electrolyte anion was changed from ClO<sub>4</sub><sup>-</sup> → Cl<sup>-</sup> → Br<sup>-</sup> → I<sup>-</sup>. For example, on Cu(100) at -1.23 V vs. RHE, as the electrolyte anion changed from ClO<sub>4</sub><sup>-</sup> to I<sup>-</sup>, the Faradaic efficiencies of ethylene (FE<sub>ethylene</sub>) improved from 31 to 50%, FE<sub>ethanol</sub> increased from 7 to 16%, and the current densities of ethylene and ethanol showed respectively 5 and 7 folds enhancement. A remarkable total FE up to 74% for C<sub>2</sub> and C<sub>3</sub> products were also obtained in the KI electrolyte. Despite their roughening in the presence of the electrolytes, the Cu(100) electrode still showed a greater propensity than Cu(111) for enhancing the formation of C<sub>2</sub> compounds. The favorable reduction of CO<sub>2</sub> to C<sub>2</sub> products in KI electrolyte was correlated with a higher \*CO population on the surface, as shown using linear sweep voltammetry. *In situ* Raman spectroscopy indicates that the coordination environment of \*CO was altered by the electrolyte anion used. Thus, apart from affecting the morphology of the electrode and local pH, we propose that the anion plays a critical role in enhancing the formation of C<sub>2</sub> products, by tuning the coordination environment of adsorbed \*CO for more efficient C-C coupling.

## Introduction

Reducing CO<sub>2</sub> emission from the use of fossil fuels is urgently needed to prevent undesirable global warming.<sup>[1]</sup> Using renewable electricity and catalysts to electroreduce CO<sub>2</sub> to chemicals and fuels offers a promising approach to reduce our reliance on fossil fuels.<sup>[2]</sup> Copper-based catalysts are particularly attractive for such a purpose, owing to their unique ability to reduce CO<sub>2</sub> to ethylene and ethanol.<sup>[3]</sup> However, the poor product selectivity and large overpotentials required by these catalysts make them inapt for industrial applications. Hence, considerable resources have been invested to tune the structure of the Cu catalysts, and their electrochemical environment, in order to optimize their CO<sub>2</sub>-to-C<sub>2</sub> selectivity.

The activity of Cu catalysts for the CO<sub>2</sub> reduction reaction (CO<sub>2</sub>RR) is influenced by their surface orientation,<sup>[4]</sup> grain boundaries,<sup>[5]</sup> type of electrolytes used,<sup>[6]</sup> etc. The importance of electrolyte cation was first reported by Hori et al.<sup>[6f]</sup> An increase in the selectivities for CO, ethylene and ethanol production on

copper electrodes was observed as the sizes of the cations (from Li<sup>+</sup> to Cs<sup>+</sup>) used increased. This effect was also found by Kenis and Bell for the electroreduction of CO<sub>2</sub> to CO on silver electrodes.<sup>[6b, 7]</sup> Bell's group further investigated the role of the electrolyte cation by modeling the local pH and electric field near the cathode.<sup>[6b, 6c]</sup> Due to the consumption of protons (supplied from water dissociation) during CO<sub>2</sub>RR and hydrogen evolution, the pH at the surface of the working electrode is expected to rise.<sup>[3]</sup> However, larger cations, especially Cs<sup>+</sup>, are also predicted to hydrolyze easily ([Cs(H<sub>2</sub>O)<sub>n</sub>]<sup>+</sup> + H<sub>2</sub>O → [Cs(H<sub>2</sub>O)<sub>n-1</sub>(OH)] + H<sub>3</sub>O<sup>+</sup>), and their use will buffer the rise of local pH.<sup>[6b]</sup> The resultant lowered local pH will facilitate the dissolution of CO<sub>2</sub> near the cathode and consequently enhance the CO<sub>2</sub> reduction activity. It was further suggested that hydrated Cs<sup>+</sup> ions were more concentrated in the outer Helmholtz plane, and could induce a greater electric field to stabilize \*CO and \*OCCO adsorbates, the key intermediates for ethylene and ethanol production.<sup>[6c]</sup>

The effect of electrolyte anion has also been investigated for CO<sub>2</sub>RR.<sup>[6a, 6d, 6e]</sup> Hori et al. reported higher selectivities towards ethylene on polycrystalline Cu electrodes in non-buffering KCl, KClO<sub>4</sub> and K<sub>2</sub>SO<sub>4</sub> electrolytes, as compared to buffers such as KHCO<sub>3</sub> and K<sub>2</sub>HPO<sub>4</sub>.<sup>[6a, 8]</sup> Local pHs are expected to rise higher when electrolytes with lower buffering abilities are used. Thus, Hori attributed the higher ethylene selectivities detected in the non-buffering electrolytes to the higher local pHs at the electrode surface.<sup>[6a]</sup> This can be rationalized in terms of the decoupled proton-electron transfer step that occurs during the formation of ethylene. Subsequently, the Ogura group reported selective ethylene formation on copper electrodes coated with Cu halide in concentrated (3 M) potassium halide electrolytes.<sup>[9]</sup> Of the three halides (Cl<sup>-</sup>, Br<sup>-</sup> and I<sup>-</sup>) used, Br<sup>-</sup> most favored ethylene production. The halide was proposed to aid the adsorption of CO<sub>2</sub> via charge transfer and stabilize the pertinent carboxyl (COOH) intermediates. The absence of infrared spectroscopic signals belonging to adsorbed CO also led them to propose that this species is not involved in the formation of ethylene.<sup>[9a]</sup> Roldan-Cuenya et al. performed CO<sub>2</sub> reduction on preoxidized Cu catalysts in KHCO<sub>3</sub> electrolytes mixed with KCl, KBr or KI (non-buffers).<sup>[6e]</sup> Therein, the current densities of ethylene and ethanol increased as the anion was changed from Cl<sup>-</sup> → Br<sup>-</sup> → I<sup>-</sup>.<sup>[6e]</sup> The higher selectivity and activity for C<sub>2</sub> products observed on these electrodes (compared to a copper foil reference) was not attributed to significant changes in local pHs as a KHCO<sub>3</sub>-based buffer was used. The change in activity was instead ascribed to effects from the adsorbed halide anion, subsurface oxygen and roughened surface. Here, we note that both Cu halides and preoxidized Cu electrodes are already known to promote the formation of C<sub>2</sub> products.<sup>[6e, 9a, 10]</sup> Thus, it is difficult to clarify the role of the electrolyte anion on the selectivity of CO<sub>2</sub>RR.

[a] Y. Huang, C.W. Ong, Prof. Dr. B.S. Yeo  
Department of Chemistry, National University of Singapore  
3 Science Drive 3, Singapore 117543  
E-mail: chmyeos@nus.edu.sg

Supporting information for this article is given via a link at the end of the document. ((Please delete this text if not appropriate))

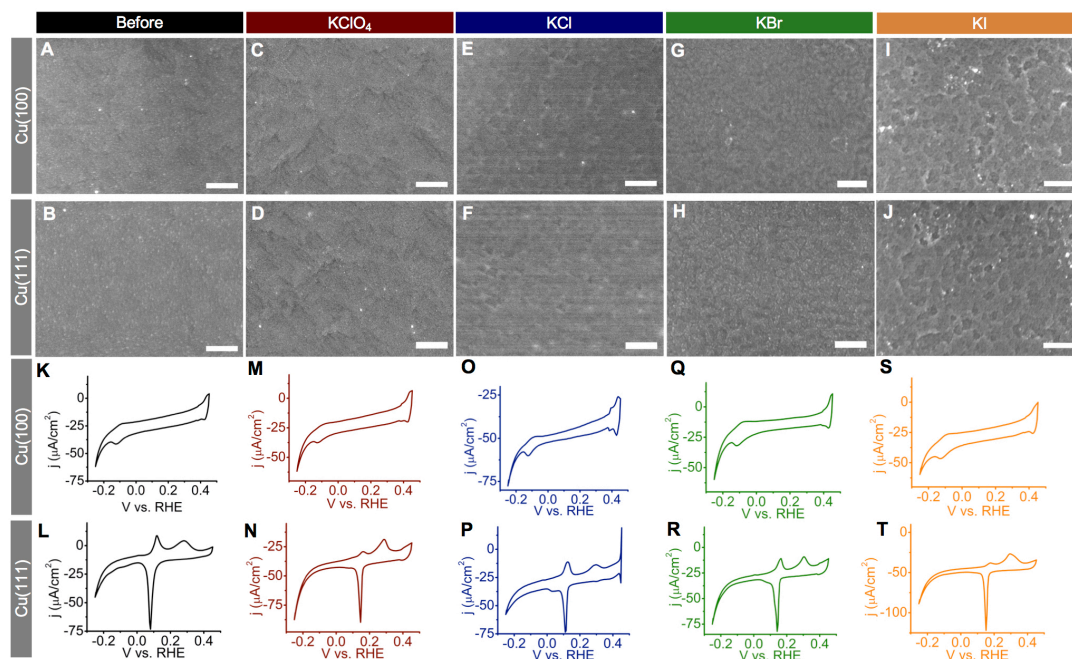


**Figure 1.** Scanning electron micrographs of Cu(100) and Cu(111) electrodes (A-B) before CO<sub>2</sub> reduction; after CO<sub>2</sub> reduction in (C-D) KClO<sub>4</sub>, (E-F) KCl, (G-H) KBr and (I-J) KI electrolytes at -1.23 V vs. RHE. Scale bar: 500 nm. (K-T) The corresponding cyclic voltammograms of the same electrodes (in N<sub>2</sub>-saturated 0.1 M KOH, scan rate of 50 mV/s).

In this work, we examine the product distribution of CO<sub>2</sub> reduction on Cu(100) and Cu(111) electrodes in non-buffering KClO<sub>4</sub>, KCl, KBr and KI electrolytes. The formation of ethylene and ethanol increased on both surfaces as the electrolyte anion was varied from ClO<sub>4</sub><sup>-</sup> → Cl<sup>-</sup> → Br<sup>-</sup> → I<sup>-</sup>. Effects of morphology and local pH were examined. Linear sweep voltammetry and Raman spectroscopy were also used to probe the anion's effect on CO adsorption on Cu. The effect of the anion on the formation of C<sub>2</sub> compounds is discussed.

## Results and Discussion

### Characterization of the electrodes before and after CO<sub>2</sub> reduction

Scanning electron microscopy (SEM) of freshly-prepared Cu(100) and Cu(111) electrodes showed that their surfaces were smooth (Figure 1). Their cyclic voltammograms (CV) were consistent with previous studies, as evidenced by their OH<sup>-</sup> adsorption/desorption peaks located between -0.2 and 0.3 V vs. RHE (all potentials cited in this work are referenced to the reversible hydrogen electrode).<sup>[11]</sup>

CO<sub>2</sub> reduction was then performed on these surfaces for 40 min in 0.1 M KClO<sub>4</sub>, KCl, KBr and KI electrolytes at a representative potential of -1.23 V. SEM images of these surfaces after CO<sub>2</sub>RR revealed their roughening, especially when electrolysis were performed in KBr and KI electrolytes (Figure 1G-J).<sup>[6d]</sup> We could not discern any differences between the way the two surfaces were roughened in each electrolyte. Double-layer capacitance measurements showed that these

surfaces had up to 1.6× larger surface roughness factors than those before CO<sub>2</sub> reduction (Table S1 of the Supporting Information). The surface roughening could be due to formation of CuBr/CuI particles on the Cu surfaces upon their contact with electrolytes at open circuit condition, followed by their reduction during CO<sub>2</sub> electrolysis (Figure S1 of the Supporting Information).<sup>[6e]</sup> Interestingly, the CVs of the Cu electrodes after CO<sub>2</sub>RR resembled those of freshly-prepared ones (Figure 1K-T). This indicates that the surface orientation of the Cu single crystals were largely maintained after electrolysis, consistent with additional results from high resolution and 2D X-ray diffraction analyses of the electrodes (Figures S2 and S3 of the Supporting Information).

### Distribution of CO<sub>2</sub> reduction products on Cu(100) and Cu(111) surfaces

CO<sub>2</sub> reduction was performed on Cu(100) and Cu(111) electrodes at potentials between -0.98 and -1.38 V in 0.1 M KClO<sub>4</sub>, KCl, KBr and KI electrolytes. The products were analyzed using gas and liquid chromatography (Figures S4 and S5 of the Supporting Information). The data is grouped based on our products of interest, which are CO, formate, ethylene, ethanol and CH<sub>4</sub> (Figures 2 and 3, Figure S6 of the Supporting Information). The FEs for other products including hydrogen, n-propanol, etc. are listed in Tables S2-9 of the Supporting Information.

### Cu(100)

Starting at a potential of -0.98 V, CO production on Cu(100) was favored in KI over KClO<sub>4</sub> electrolyte (Figure 2A-B).

Specifically, when the electrolyte was switched from  $\text{KClO}_4$  to KI,  $\text{FE}_{\text{CO}}$  increased from 11.8% to 22.8% and the corresponding  $j_{\text{CO}}$  doubled from  $-0.06$  to  $-0.12$   $\text{mA}/\text{cm}^2$ . At  $-1.08$  V, ethylene and ethanol production increased while CO evolution decreased (Figure 2C-F). These observations indicate that CO is an intermediate for the formation of these C2 products.<sup>[12]</sup>

The selectivity towards ethylene peaked at  $-1.23$  V in all four electrolytes, with  $\text{FE}_{\text{ethylene}}$  of 50.3% in KI and  $\text{FE}_{\text{ethylene}}$  of 30.6% in  $\text{KClO}_4$  (Figure 2C-D). In KI electrolyte, the optimum  $j_{\text{ethylene}}$  reached  $-6.06$   $\text{mA}/\text{cm}^2$ , which was 5 times higher than

that in  $\text{KClO}_4$  ( $-1.20$   $\text{mA}/\text{cm}^2$ ). The enhancement in ethanol production follows the same trend as that of ethylene (Figure 2E-F). At  $-1.23$  V, the optimized  $\text{FE}_{\text{ethanol}}$  increased from 7.1% to 16.4% and the corresponding  $j_{\text{ethanol}}$  improved from  $-0.28$  to  $-1.98$   $\text{mA}/\text{cm}^2$  when switching electrolytes from  $\text{KClO}_4$  to KI.

It is noteworthy that the total FEs for C2 and C3 products at  $-1.23$  V reached as high as 74 % in KI electrolyte. This value is the state-of-the-art as compared to those reported for plasma-activated Cu ( $\text{FE}_{\text{C}_2\text{-C}_3} = \sim 65\%$ ),<sup>[6e]</sup> Cl-induced  $\text{Cu}_2\text{O-Cu}$  ( $\text{FE}_{\text{C}_2\text{-C}_3} = \sim 60\%$ )<sup>[13]</sup> and oxide-derived Cu catalysts ( $\text{FE}_{\text{C}_2\text{-C}_3} = \sim 70\%$ ).<sup>[14]</sup>

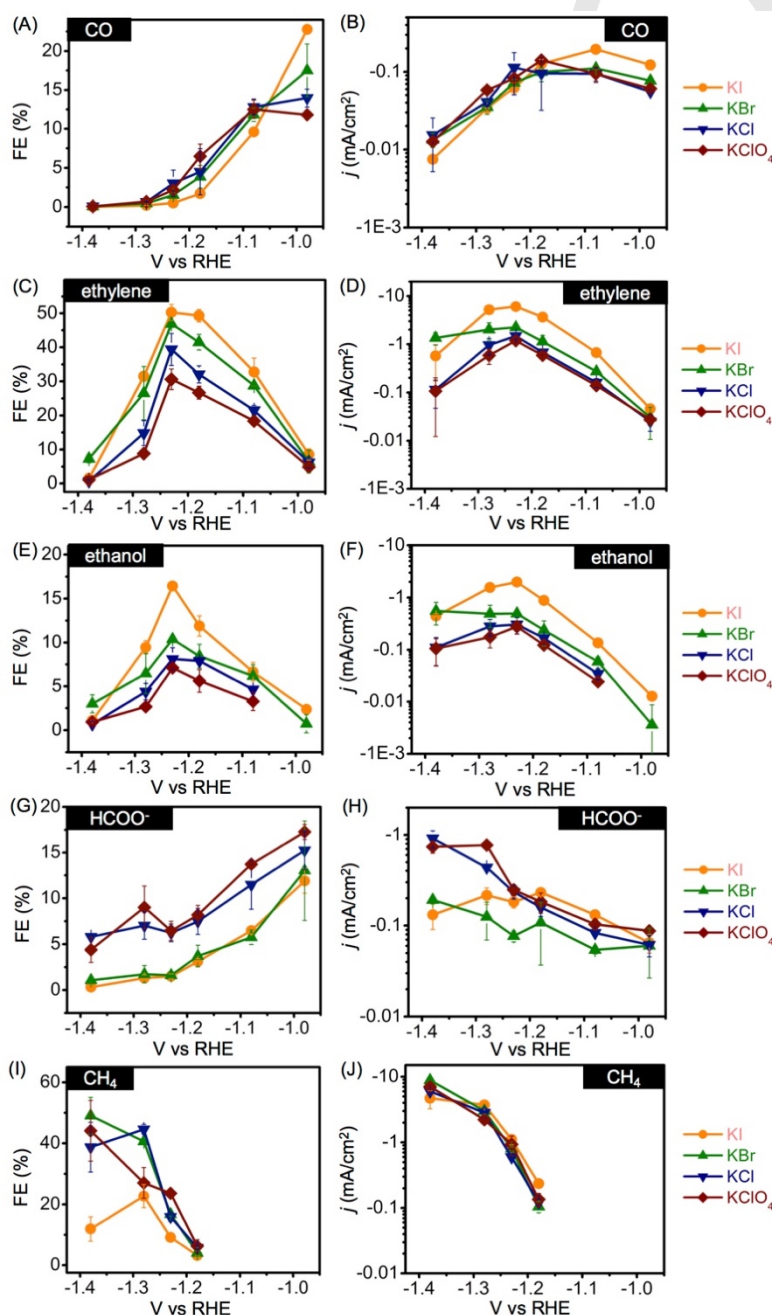


**Figure 2.** Faradaic efficiencies and partial current densities for (A-B) CO, (C-D) ethylene, (E-F) ethanol, (G-H)  $\text{HCOO}^-$  and (I-J)  $\text{CH}_4$  produced on Cu(100) in 0.1 M  $\text{KClO}_4$ , KCl, KBr and KI electrolytes at various applied potentials.

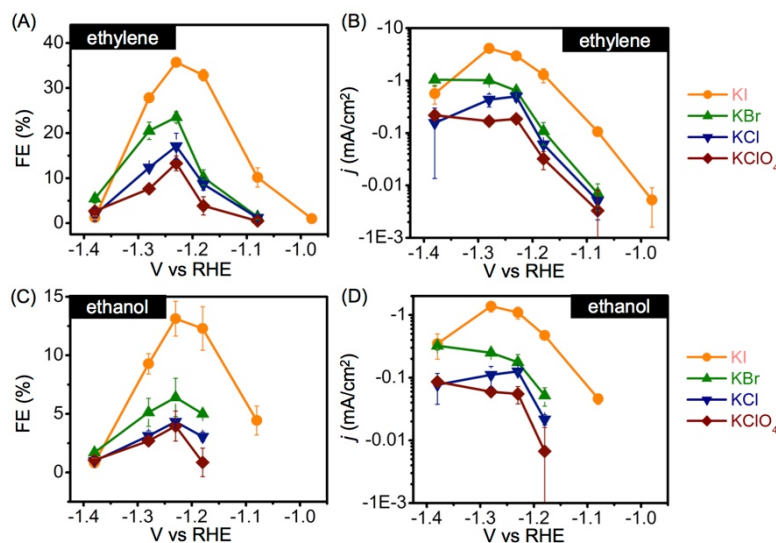


**Figure 3.** Faradaic efficiencies and partial current densities for (A-B) ethylene and (C-D) ethanol produced on Cu(111) in 0.1 M KClO<sub>4</sub>, KCl, KBr and KI electrolytes at various applied potentials.

Selectivity towards formate is less favored in KBr/KI as compared to KClO<sub>4</sub> electrolytes (Figure 2G-H). At -0.98 V, the  $FE_{\text{formate}}$  reduced from 17.3% in KClO<sub>4</sub> to 11.9% in KI electrolyte, in contrast to the enhancement of CO and ethylene production observed at the same conditions. This can be ascribed to the competing production of formate and CO (and its further reduced products).<sup>[15]</sup>

At potentials negative to -1.28 V, Cu(100) became selective for CH<sub>4</sub> production in KClO<sub>4</sub>, KCl and KBr electrolytes (Figure 2I-J). The highest  $FE_{\text{CH}_4}$  of 49.1% was obtained in KBr electrolyte at -1.38 V, while a highly suppressed  $FE_{\text{CH}_4}$  of 11.9% was found in KI electrolyte at the same potential. Despite the generally suppressed  $FE_{\text{CH}_4}$  in KI, the geometric current density for CH<sub>4</sub> in KI is comparable to that in the KBr system. This is likely due to the increased surface roughness of the Cu electrode in KI electrolytes.

### Cu(111)

The trend in which C2 products are formed on Cu(111) in different electrolytes is similar to that described on Cu(100). Changing the electrolyte from KClO<sub>4</sub> to KI increased the optimum  $FE_{\text{ethylene}}$  from 13.3 to 35.7% and the corresponding  $j_{\text{ethylene}}$  from -0.19 to -2.96 mA/cm<sup>2</sup> (Figure 3A-B). The FE and current densities of ethanol also improved (Figure 3C-D).

It is noteworthy that though Cu(100) and Cu(111) were visibly roughened during CO<sub>2</sub> electrolysis, their original surface crystallographies were largely preserved (Figure 1, Figures S2 and S3). This could explain the higher ethylene selectivity observed on Cu(100) as compared to on Cu(111). Such a surface structure effect has been confirmed by density functional theory (DFT) calculations and by performing CO<sub>2</sub> reduction on Cu foils, whose exposed facets are tuned using metal ion cycling.<sup>[16]</sup> The propensity of Cu(100) electrodes to reduce CO<sub>2</sub> to ethylene has also been attributed to the presence of a high \*CO coverage on the electrode during CO<sub>2</sub>RR, which lowered

the activation barrier for CO dimerization.<sup>[4a, 17]</sup> The potential-dependent production of CO, formate and CH<sub>4</sub> on Cu(111) in the four electrolytes were similar to that observed on Cu(100) (Figure S6 of the Supporting Information).

### Factors responsible for the C2 enhancement

We now investigate the reasons behind the increased formation of ethylene and ethanol as the electrolyte anion was changed from ClO<sub>4</sub><sup>-</sup> → Cl<sup>-</sup> → Br<sup>-</sup> → I<sup>-</sup>. Is it due to electrode roughening, rise in local pH induced from the non-buffering electrolytes, or the anion's role in tuning the \*CO adsorption environment?

### Morphological factor

A Cu(100) electrode was used for two consecutive CO<sub>2</sub> reductions (each for 40 min) at -1.23 V, first in KI and then in KClO<sub>4</sub> electrolyte. The production of C2 compounds in KI was significantly reduced during the second electrolysis in KClO<sub>4</sub> (Table 1, Table S10 of the Supporting Information). Specifically, the  $FE_{\text{ethylene}}$  and  $FE_{\text{ethanol}}$  decreased respectively from 50.3 to 37.2% and 16.4 to 10.0%. Nonetheless, the production of ethanol and ethylene at the 2<sup>nd</sup> electrolysis [i.e., KI-treated Cu(100) in KClO<sub>4</sub>] is still higher than that shown by a fresh Cu(100) in KClO<sub>4</sub> electrolyte ( $FE_{\text{ethylene}} = 30.6\%$ ,  $FE_{\text{ethanol}} = 7.1\%$  at -1.23 V). Its total current density is also larger by 1.5×. This enhancement (in the production of C2 compounds) can be attributed to the more extensive roughening of its surface after the 1<sup>st</sup> electrolysis in KI electrolyte. However, it is significantly smaller than the enhancement observed using only KI as the electrolyte. Therefore, we conclude that while a rough Cu surface may contain catalytically-active defect sites for reducing CO<sub>2</sub> to C2 products, the morphology itself cannot be the sole responsible factor.

### Local pH

The electrolytes used in this work are non-buffers.<sup>[8]</sup> Previous

**Table 1:** Faradaic efficiencies for CO<sub>2</sub> reduction products formed on Cu(100) during sequential CO<sub>2</sub> reductions in 0.1 M KI and 0.1 M KClO<sub>4</sub> electrolytes, and Cu(100) in 0.1 M KClO<sub>4</sub> electrolyte. All experiments were performed at -1.23 V for 40 min.

$j_{\text{tot}}$ (mA/cm <sup>2</sup> )	Faradaic Efficiency (%)							Total
	CH <sub>4</sub>	C <sub>2</sub> H <sub>4</sub>	CO	H <sub>2</sub>	EtOH	HCOO <sup>-</sup>	Other liquid products <sup>[a]</sup>	
	<b>1<sup>st</sup> electrolysis of Cu(100) in KI</b>							
-12.06	9.2	50.3	0.5	19.9	16.4	1.5	7.1	104.9
	<b>2<sup>nd</sup> electrolysis of Cu(100) in KClO<sub>4</sub></b>							
-5.89	28.3	37.2	1.5	14.1	10.0	4.8	6.0	101.9
	<b>Cu(100) in KClO<sub>4</sub></b>							
-3.93	23.6	30.6	2.2	28.3	7.1	6.5	5.1	103.5

[a]: Other liquid products include acetaldehyde, propionaldehyde, methanol, ally alcohol and n-propanol. The standard deviations of the measurements have been listed in Table S10 of the Supporting Information

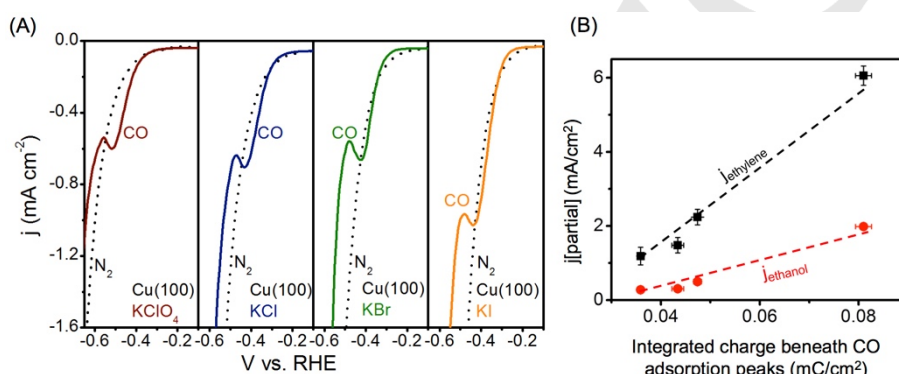


**Figure 4.** (A) Linear sweep voltammograms of Cu(100) electrodes in 0.1 M KClO<sub>4</sub>, KCl, KBr and KI electrolytes saturated in CO (solid lines) and N<sub>2</sub> (dotted lines). Scan rate = 10 mV/s. (B) Correlation between the integrated charges beneath CO adsorption peaks (from a) and the partial current densities for ethylene (black) and ethanol (red) produced on Cu(100) at -1.23 V in the four electrolytes.

studies have shown that local pH is dependent on the applied current densities.<sup>[18]</sup> Herein, we model the local pH within the diffusion layer using Gupta's model.<sup>[18a, 19]</sup> As expected, the pH rises when going from bulk electrolyte to the surface of the Cu(100) during CO<sub>2</sub> reduction at -1.23 V (Table S11 and Figure S7 of the Supporting Information). Experimentally, Cu(100) in KI electrolytes exhibited the largest current densities. Thus, its surface pH (pH 11.0) was calculated to be the highest as compared to those electrodes held in the other three electrolytes (pHs between 10.3 and 10.4).

To investigate the effect of local pH on ethylene formation, we analyzed the Faradaic efficiencies for ethylene on Cu(100) in the four electrolytes at -1.23 V against the calculated surface pH values (Figure S8 of the Supporting Information). Interestingly, while KClO<sub>4</sub>, KCl and KBr electrolyte systems shared similar surface pHs at ~10.4, the spread of their FE<sub>ethylene</sub> values varied greatly from 30.6 to 46.9%. The weak correlation of local pH and FE<sub>ethylene</sub> suggests that local pH is not a dominant factor for enhancing the formation of C<sub>2</sub> products during CO<sub>2</sub>RR in KClO<sub>4</sub>, KBr and KCl electrolytes.

#### Role of anion

**CO adsorption on Cu single crystals:** The adsorption of CO on Cu in different electrolytes was probed by linear sweep voltammetry (Figure 4A and Figure S9 of the Supporting

Information). By comparing the cathodic currents on Cu(100) in CO- and N<sub>2</sub>-saturated electrolytes, we noted that the onsets of H<sub>2</sub> evolution were delayed under CO environment (by 44-87 mV at -1.2 mA/cm<sup>2</sup>). We attribute this to the presence of adsorbed \*CO which blocks available sites for HER and also weakens Cu-H bonding.<sup>[20]</sup> Copper's HER activity will thus be lower as it lies on the right-hand (weak-binding) side of the HER volcano plot.<sup>[20a]</sup>

Reduction peaks also appeared at approx. -0.45 V during the cathodic scans of Cu(100) in CO-saturated 0.1 M KClO<sub>4</sub>, KCl, KBr and KI electrolytes (Figure 4A). These peaks could be ascribed to CO adsorbed onto Cu(100) accompanied by electron transfer.<sup>[19, 20b, 21]</sup> In support of this, we note that the first CO reduction product, ethylene, was observed only at -0.76 V on the same surface in CO-saturated KI electrolyte (Table S12 of the Supporting Information). Roberts et al. had also reported an onset potential of -0.5 V vs. RHE for CO reduction on Cu(100) in pH 7 electrolyte.<sup>[21b]</sup>

The integrated charges of the CO adsorption peaks (which increased as the electrolyte anion was changed from ClO<sub>4</sub><sup>-</sup> → Cl<sup>-</sup> → Br<sup>-</sup> → I<sup>-</sup>) are associated with the population of \*CO on the Cu surface. Interestingly, when the current densities of ethylene and ethanol obtained on a Cu(100) surface at -1.23 V was plotted against these charges, a linear correlation was observed (Figure 4B). This indicates that enhancement in C<sub>2</sub> products is linked to

the increased \*CO population on the electrode. This result agrees with our previous studies of CO adsorption on CuCl-derived Cu mesocrystals, Cu nanoparticles and polycrystalline Cu surfaces.<sup>[19, 22]</sup> Therein, we found that catalysts, which exhibited good selectivity towards CO<sub>2</sub> reduction to ethylene, adsorb CO most readily. We further highlight that Verdaguer-Cassadevall et al. have reported the presence of strongly chemisorbed CO on Cu catalysts active for the reduction of CO<sub>2</sub> to C<sub>2</sub> compounds.<sup>[23]</sup>

We note that the LSVs of Cu(111) did not show the charge transfer peak (Figure S9 of the Supporting Information). This is consistent with previous findings by Hori et al.<sup>[20b]</sup> Nonetheless, suppression in HER was similarly observed in the order of ClO<sub>4</sub><sup>-</sup> < Cl<sup>-</sup> < Br<sup>-</sup> < I<sup>-</sup>.

**\*CO binding environment on Cu single crystals probed by *in situ* Raman spectroscopy:** *In situ* Raman spectroscopy was performed on copper in CO<sub>2</sub>-saturated 0.1 M KX (X = ClO<sub>4</sub><sup>-</sup>, Cl<sup>-</sup>, Br<sup>-</sup> and I<sup>-</sup>) electrolytes (Figure 5 and Figure S10 of the Supporting Information). Mechanically polished polycrystalline Cu was used for this purpose as we found it easier to focus the Raman laser tightly on this surface as compared to the smooth single crystal surface. The working potential was set at -0.98 V, where strong CO production is expected (Figure 2 and Figure S6 of the Supporting Information).

Only Raman bands at 280, 365 and ~2060-2090 cm<sup>-1</sup> were recorded (Figure 5). These can be assigned respectively to the Cu-CO frustrated rotation, Cu-CO stretching and C=O stretching

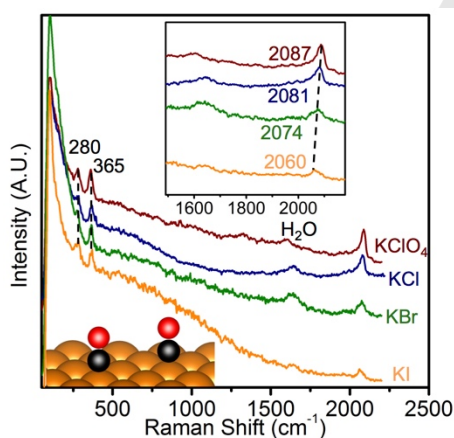


**Figure 5.** *In situ* Raman spectra of polycrystalline Cu cathode during electrochemical reduction of CO<sub>2</sub> in KClO<sub>4</sub>, KCl, KBr and KI electrolytes at -0.98 V. The top Insert shows the red shifting of the C=O stretching bands in the order of ClO<sub>4</sub><sup>-</sup> < Cl<sup>-</sup> < Br<sup>-</sup> < I<sup>-</sup>, and the bottom Insert presents a schematic illustration of CO adsorbed on the Cu surface.

modes of adsorbed \*CO.<sup>[24]</sup> Interestingly, the stretching vibration of C=O decreased from 2087 to 2060 cm<sup>-1</sup>, when the electrolyte was changed from KClO<sub>4</sub> to KI. The weakening of C=O stretching indicates that the coordination environment of CO was altered by the presence of different anions.

Although CO production was strongest in KI electrolyte at -0.98 V (Figure 2 and Figure S6 of the Supporting Information), its \*CO Raman bands did not show the highest intensities. This could be related to the roughening of the surface, which affects the optical properties of the surface. Additionally, no peaks corresponding to Cu-I (~125/~140 cm<sup>-1</sup>) or Cu-Br (~135/~170 cm<sup>-1</sup>) could be discerned,<sup>[25]</sup> as they were obscured by the background peak at ~100 cm<sup>-1</sup>. We also could not detect signals belonging to further reduced species, which can be attributed to the insufficient limits of detection afforded by our spectrometer.

**Effects of anions on C2 production:** In this work, the formation of ethylene and ethanol on Cu(100) and Cu(111) surfaces generally increase as the electrolyte anion was changed from ClO<sub>4</sub><sup>-</sup> → Cl<sup>-</sup> → Br<sup>-</sup> → I<sup>-</sup>. This trend mirrors that of the binding abilities of the anions on Cu in the order of ClO<sub>4</sub><sup>-</sup> < Cl<sup>-</sup> < Br<sup>-</sup> < I<sup>-</sup>.<sup>[26]</sup> The Cu(100) facet was also shown better than Cu(111) in enhancing the formation of C2 products.

We acknowledge that the electrolyte anions might compete with active CO<sub>2</sub>RR intermediates for adsorption sites. However, our LSV results suggest that \*CO adsorption on Cu surface was actually enhanced by the co-adsorbed anions. The resultant high population of \*CO could then in turn facilitate C-C coupling of the CO intermediates to C2 products.<sup>[4a, 17a]</sup> Our hypothesis is supported by Shaw et al., who revealed using DFT calculations, that the \*CO binding energy on Cu can be increased by up to 0.2 eV in the presence of co-adsorbed anions (F<sup>-</sup> and Cl<sup>-</sup>).<sup>[21a]</sup> It is noteworthy that an infrared spectroscopy study by Scarano et al. demonstrated the greater ability of CuCl surface to bind to CO.<sup>[27]</sup> Our propositions also agree well with recent DFT calculations by Nørskov and our group, which showed that increasing \*CO coverage on Cu surfaces lowers the energy barrier for C-C coupling.<sup>[4a, 17a]</sup>

Additionally, the adsorbed anion could modify the electronic structure of the local Cu sites, which could induce a more positive charge on carbon atom of \*CO adsorbate. Anion-free copper sites, on the other hand, tend to promote π-back donation (from Cu) into the antibonding 2π\* orbital of \*CO,<sup>[28]</sup> resulting in a more negatively charged carbon atom of \*CO adsorbate. The electrostatic attraction between the oppositely charged carbon atoms could render stability to the CO dimerization product and in turn facilitate the C-C coupling process. Goddard et al. have similarly attributed the enhanced formation of C2 products on Cu<sub>2</sub>O-derived Cu surface to the electrostatic stabilization between two carbon atoms induced by Cu<sup>+</sup> and Cu<sup>0</sup> interface.<sup>[29]</sup> Their DFT calculations suggest such stabilization could improve the thermodynamics and kinetics of CO dimerization.

Hori et al. first reported the use of non-buffers for enhancing the formation of C2 products and the improved performance was attributed to the rise of local pH at the working electrode surface.<sup>[8]</sup> Roldan Cuenya et al. further demonstrated increased CO<sub>2</sub> reduction rate on preoxidized Cu electrodes in halide containing KHCO<sub>3</sub> buffers,<sup>[6e]</sup> and factors including subsurface oxygen, anion adsorption and surface roughening were proposed for the enhancement. In this work, we have demonstrated that the enhancement in ethylene and ethanol

production (in terms of both Faradaic efficiencies and partial current densities) strongly correlates with the population of \*CO on the surface. The presence of the adsorbed anion, specifically I<sup>-</sup>, is suggested to be a dominant cause for the enhancement. We show that the catalytic selectivity and activity of electrochemical reduction of CO<sub>2</sub> can be tuned by the judicious selection of appropriate electrolyte anion.

## Conclusions

We have examined the electroreduction of CO<sub>2</sub> on Cu(100) and Cu(111) surfaces in 0.1 M KClO<sub>4</sub>, KCl, KBr and KI electrolytes. The formation of ethylene and ethanol on these surfaces was enhanced when the anion of the electrolyte was varied in the order of ClO<sub>4</sub><sup>-</sup> → Cl<sup>-</sup> → Br<sup>-</sup> → I<sup>-</sup>. The use of KI as the electrolyte yielded the highest FE<sub>ethylene</sub> of 50% and FE<sub>ethanol</sub> of 16%, and with the total FE for C2-C3 products reaching 74% at -1.23 V. Apart from affecting the surface morphologies and local pHs of the electrodes, we propose that the electrolyte anion can facilitate a higher population of adsorbed \*CO, which thus promotes their C-C coupling to C2 products.

## Experimental Section

**Electrode preparation and characterization:** Cu(100) and Cu(111) single-crystal surfaces (99.99%, 10 mm diameter, MTI Corp.) were prepared through mechanical polishing, electropolishing and acid rinsing in 0.1 mM HClO<sub>4</sub> solution.<sup>[30]</sup> The surface morphology of the electrodes was characterized using scanning electron microscopy (JEOL JSM-6710 F, 5 kV, 10 μA). Their surface orientation were checked by cyclic voltammetry in 0.1 M KOH,<sup>[11]</sup> as well as high resolution and 2D X-ray diffraction. The surface roughness factors of these electrodes after CO<sub>2</sub> reduction were estimated using their double-layer capacitances. CO adsorption on the Cu single-crystal surfaces was examined by linear sweep voltammetry.<sup>[4b]</sup> An Autolab PGSTAT100 potentiostat was used for controlling the aforementioned electrochemistries. *In situ* Raman spectroscopy (Horiba Jobin Yvon) was performed to probe the structure of the \*CO intermediates on mechanically polished polycrystalline Cu surfaces. A He-Ne laser (633 nm, CVI Melles Griot) was employed as the excitation source. A water-immersion objective (Olympus LUMFL, 60×, numerical aperture = 1.10) protected with an optically transparent Teflon film (0.013 mm, American Durafilm) was used during the *in situ* electrochemical measurements.

**Electrochemical reduction of CO<sub>2</sub>:** 0.1 M KClO<sub>4</sub> (99.99%, Sigma-Aldrich), KCl (99.99%, Sigma-Aldrich), KBr (99.95%, Meryer Chemical) and KI (99.99%, Meryer Chemical) electrolytes were prepared with ultrapure water (Type I, Barnstead, Thermo Scientific). We employed a two-compartment electrochemical cell,<sup>[31]</sup> separated by a cation-exchange membrane (Selemon CMV, AGC Asahi Glass), to perform CO<sub>2</sub>/CO chronoamperometric measurements using a Gamry Reference 600 potentiostat. 20 sccm of CO<sub>2</sub> (99.999%, Linde Gas) or 5 sccm of CO (99.9%, Linde Gas) were purged into the two compartments during the 40 min electrolysis. A Ag/AgCl electrode (Saturated KCl, Pine Research Instrumentation) and a Pt wire (ALS Japan) were employed as reference and counter electrodes respectively. The current interrupt mode was used for compensating the iR drop. All potentials reported here were referenced to the RHE. The pHs were measured to be ~3.8 for CO<sub>2</sub>-saturated KClO<sub>4</sub>, KCl, KBr and KI solutions and 5.8 for CO-saturated KI

solution. The gas products were periodically analyzed by gas chromatography (GC, 7890A, Agilent). Liquid products were collected after chronoamperometry and quantified using headspace gas chromatography (HSGC, Agilent, 7890B) and high-performance liquid chromatography (HPLC, Agilent, 1260 Infinity). The product distribution reported here is the average of at least three independent measurements at each potential. All the currents were normalized to the exposed geometric surface area (0.385 cm<sup>2</sup>) of the working electrode.

**Modeling of local pH:** A steady-state 1-D modeling in MATLAB 8.5 was performed to calculate the local pH within the diffusion layer in various electrolytes, and to investigate its effect on C2 production.<sup>[18a, 19]</sup>

## Acknowledgements

This work is supported by a research fund (R-143-000-683-112) from the Ministry of Education, Singapore. Y.H. and C.W.O. acknowledge Ph.D. research scholarships from the Ministry of Education, Singapore. We thank Dr. Albertus D. Handoko (Institute of Materials Research and Engineering) for the XRD measurements.

**Keywords:** carbon dioxide reduction • copper single crystals • anion • ethylene • ethanol

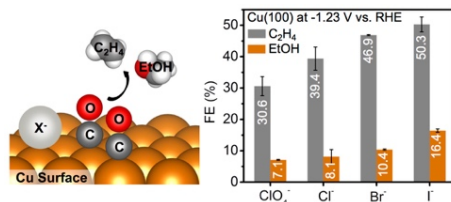
- [1] P. Friedlingstein, R. M. Andrew, J. Rogelj, G. P. Peters, J. G. Canadell, R. Knutti, G. Luderer, M. R. Raupach, M. Schaeffer, D. P. van Vuuren, C. Le Quére, *Nat. Geosci.* **2014**, *7*, 709-715.
- [2] D. Ren, N. W. X. Loo, L. Gong, B. S. Yeo, *ACS Sustainable Chem. Eng.* **2017**, *5*, 9191-9199.
- [3] M. Gattrell, N. Gupta, A. Co, *J. Electroanal. Chem.* **2006**, *594*, 1-19.
- [4] a) Y. Huang, A. D. Handoko, P. Hirusit, B. S. Yeo, *ACS Catal.* **2017**, *7*, 1749-1756; b) Y. Hori, I. Takahashi, O. Koga, N. Hoshi, *J. Mol. Catal. A: Chem.* **2003**, *199*, 39-47.
- [5] X. Feng, K. Jiang, S. Fan, M. W. Kanan, *J. Am. Chem. Soc.* **2015**, *137*, 4606-4609.
- [6] a) Y. Hori, A. Murata, R. Takahashi, *J. Chem. Soc., Faraday Trans. 1* **1989**, *85*, 2309-2326; b) M. R. Singh, Y. Kwon, Y. Lum, J. W. Ager, A. T. Bell, *J. Am. Chem. Soc.* **2016**, *138*, 13006-13012; c) J. Resasco, L. D. Chen, E. Clark, C. Tsai, C. Hahn, T. F. Jaramillo, K. Chan, A. T. Bell, *J. Am. Chem. Soc.* **2017**, *139*, 11277-11287; d) A. S. Varela, W. Ju, T. Reier, P. Strasser, *ACS Catal.* **2016**, *6*, 2136-2144; e) D. Gao, F. Scholten, B. Roldan Cuenya, *ACS Catal.* **2017**, *7*, 5112-5120; f) A. Murata, Y. Hori, *Bull. Chem. Soc. Jpn.* **1991**, *64*, 123-127.
- [7] M. R. Thorson, K. I. Siil, P. J. A. Kenis, *J. Electrochem. Soc.* **2013**, *160*, F69-F74.
- [8] Y. Hori, in *Modern Aspects of Electrochemistry*, Vol. 42 (Eds.: C. G. Vayenas, R. E. White, M. E. Gamboa-Aldeco), Springer New York, New York, NY, **2008**, pp. 89-189.
- [9] a) K. Ogura, *J. CO<sub>2</sub> Util.* **2013**, *1*, 43-49; b) H. Yano, T. Tanaka, M. Nakayama, K. Ogura, *J. Electroanal. Chem.* **2004**, *565*, 287-293.
- [10] D. Gao, I. Zegkinoglou, N. J. Divins, F. Scholten, I. Sinev, P. Grosse, B. Roldan Cuenya, *ACS Nano* **2017**, *11*, 4825-4831.
- [11] a) V. D. Jović, B. Jović M., *J. Serb. Chem. Soc.* **2002**, *67*, 531-546; b) K. J. P. Schouten, E. P. Gallent, M. T. M. Koper, *J. Electroanal. Chem.* **2013**, *699*, 6-9.
- [12] R. Kortlever, J. Shen, K. J. P. Schouten, F. Calle-Vallejo, M. T. M. Koper, *J. Phys. Chem. Lett.* **2015**, *6*, 4073-4082.
- [13] S. Lee, D. Kim, J. Lee, *Angew. Chem., Int. Ed.* **2015**, *54*, 14701-14705.
- [14] Y. Lum, B. Yue, P. Lobaccaro, A. T. Bell, J. W. Ager, *J. Phys. Chem. C* **2017**, *121*, 14191-14203.

- [15] J. S. Yoo, R. Christensen, T. Vegge, J. K. Nørskov, F. Studt, *ChemSusChem* **2016**, *9*, 358-363.
- [16] K. Jiang, R. B. Sandberg, A. J. Akey, X. Liu, D. C. Bell, J. K. Nørskov, K. Chan, H. Wang, *Nat. Catal.* **2018**, *1*, 111-119.
- [17] a) J. H. Montoya, C. Shi, K. Chan, J. K. Nørskov, *J. Phys. Chem. Lett.* **2015**, *6*, 2032-2037; b) R. B. Sandberg, J. H. Montoya, K. Chan, J. K. Nørskov, *Surf. Sci.* **2016**, *654*, 56-62.
- [18] a) N. Gupta, M. Gattrell, B. MacDougall, *J. Appl. Electrochem.* **2005**, *36*, 161-172; b) J. Resasco, Y. Lum, E. Clark, J. Z. Zeddon, A. T. Bell, *ChemElectroChem* **2018**, *5*, 1064-1072.
- [19] A. D. Handoko, C. W. Ong, Y. Huang, Z. G. Lee, L. Lin, G. B. Panetti, B. S. Yeo, *J. Phys. Chem. C* **2016**, *120*, 20058-20067.
- [20] a) Y.-J. Zhang, V. Sethuraman, R. Michalsky, A. A. Peterson, *ACS Catal.* **2014**, *4*, 3742-3748; b) Y. Hori, H. Wakebe, T. Tsukamoto, O. Koga, *Surf. Sci.* **1995**, *335*, 258-263.
- [21] a) S. K. Shaw, A. Berná, J. M. Feliu, R. J. Nichols, T. Jacob, D. J. Schiffrin, *Phys. Chem. Chem. Phys.* **2011**, *13*, 5242-5251; b) F. S. Roberts, K. P. Kuhl, A. Nilsson, *ChemCatChem* **2016**, *8*, 1119-1124.
- [22] C. S. Chen, A. D. Handoko, J. H. Wan, L. Ma, D. Ren, B. S. Yeo, *Catal. Sci. Technol.* **2015**, *5*, 161-168.
- [23] A. Verduguer-Casadevall, C. W. Li, T. P. Johansson, S. B. Scott, J. T. McKeown, M. Kumar, I. E. L. Stephens, M. W. Kanan, I. Chorkendorff, *J. Am. Chem. Soc.* **2015**, *137*, 9808-9811.
- [24] B. D. Smith, D. E. Irish, P. Kedzierzawski, J. Augustynski, *J. Electrochem. Soc.* **1997**, *144*, 4288-4296.
- [25] J. Serrano, M. Cardona, T. M. Ritter, B. A. Weinstein, A. Rubio, C. T. Lin, *Phys. Rev. B* **2002**, *66*, 245202.
- [26] a) A. Ignaczak, J. A. N. F. Gomes, *J. Electroanal. Chem.* **1997**, *420*, 71-78; b) I. T. McCrum, S. A. Akhade, M. J. Janik, *Electrochim. Acta* **2015**, *173*, 302-309; c) O. M. Magnussen, *Chem. Rev.* **2002**, *102*, 679-726.
- [27] D. Scarano, P. Galletto, C. Lamberti, R. De Franceschi, A. Zecchina, *Surf. Sci.* **1997**, *387*, 236-242.
- [28] G. Blyholder, *J. Phys. Chem.* **1964**, *68*, 2772-2777.
- [29] H. Xiao, W. A. Goddard, T. Cheng, Y. Liu, *Proc. Natl. Acad. Sci. U. S. A.* **2017**, DOI: 10.1073/pnas.1702405114.
- [30] I. Takahashi, O. Koga, N. Hoshi, Y. Hori, *J. Electroanal. Chem.* **2002**, *533*, 135-143.
- [31] D. Ren, Y. Deng, A. D. Handoko, C. S. Chen, S. Malkhandi, B. S. Yeo, *ACS Catal.* **2015**, *5*, 2814-2821.

Entry for the Table of Contents (Please choose one layout)

## FULL PAPER

Switching the electrolyte anion from  $\text{ClO}_4^-$  to  $\text{I}^-$  improves the production of ethylene and ethanol on Cu(100) surfaces, with the highest Faradaic efficiencies of 50% for ethylene and 16% for ethanol. The high population of  $^*\text{CO}$  facilitated by the electrolyte anion greatly promotes C-C coupling to C2 products.



Y. Huang, C. W. Ong, B. S. Yeo\*

Page No. – Page No.

Effects of Electrolyte Anions on the Reduction of Carbon Dioxide to Ethylene and Ethanol on Copper (100) and (111) Surfaces

Accepted Manuscript